

On the HI Content of MaNGA Major Merger Pairs

Qingzheng Yu¹ , Taotao Fang¹, Shuai Feng^{2,3}, Bo Zhang⁴,
C. Kevin Xu^{4,5}, Yunting Wang^{1,6} and Lei Hao⁷

¹Department of Astronomy, Xiamen University, Xiamen, Fujian 361005, China;
email: fangt@xmu.edu.cn

²College of Physics, Hebei Normal University, 20 South Erhuan Road, Shijiazhuang, Hebei
050024, China

³Hebei Key Laboratory of Photophysics Research and Application, Shijiazhuang, Hebei
050024, China

⁴National Astronomical Observatories, Chinese Academy of Sciences (NAOC), Beijing 100101,
China

⁵Chinese Academy of Sciences South America Center for Astronomy, National Astronomical
Observatories, CAS, Beijing 100101, China

⁶Department of Physics and Astronomy, University of British Columbia, 6225 Agricultural
Road, Vancouver, V6T 1Z1, Canada

⁷Shanghai Astronomical Observatory, Chinese Academy of Sciences, Shanghai 200030, China

Abstract. To study the role of HI content in galaxy interactions, we select galaxy pairs and control galaxies from the SDSS-IV MaNGA IFU survey, adopting kinematic asymmetry as a new effective indicator to describe the merger stage. With archival data from the HI-MaNGA survey and new observations from the Five-hundred-meter Aperture Spherical radio Telescope (FAST), we investigate the differences in HI gas fraction (f_{HI}), star formation rate (SFR), and HI star formation efficiency (SFE_{HI}) between pairs and controls. Our results suggest that on average the HI gas fraction of major-merger pairs is marginally decreased by $\sim 15\%$ relative to isolated galaxies, and paired galaxies during pericentric passage show weakly decreased f_{HI} (-0.10 ± 0.05 dex), significantly enhanced SFR (0.42 ± 0.11 dex), and SFE_{HI} (0.48 ± 0.12 dex). We propose the marginally detected HI depletion may originate from the gas consumption in fueling the enhanced H_2 reservoir of galaxy pairs.

Keywords. Galaxy interactions, Galaxy pairs, Galaxy mergers, Interstellar atomic gas, Star formation

1. Introduction

Interactions of galaxies provide an effective way to study the impact of HI gas during galaxy evolution, as recent observations and simulations have connected galaxy mergers with the enhancement of star formation, gas regulation, triggering of AGN, and starburst (Di Matteo et al. 2007; Cox et al. 2008; Ellison et al. 2008; Satyapal et al. 2014; Hani et al. 2018). Although many studies have focused on the gas conditions and star formation during galaxy interactions, the role of HI gas is still under debate. Using different samples of merging galaxies, some observations indicate that the HI gas fractions of galaxy mergers are enhanced relative to that of isolated galaxies (Casasola et al. 2004; Janowiecki et al. 2017; Ellison et al. 2018), while others find no significant difference in HI gas fractions

(Ellison et al. 2015; Zuo et al. 2018) or decreased HI content (Hibbard & van Gorkom 1996; Georgakakis et al. 2000). The confusing results may have been caused by several factors; for example, limited pair sample or lack of robust control sample (Moreno et al. 2019). However, the lack of rigorously defined merger stages is less explored in previous studies.

Considering the pair selection mainly relies on the projected separation (d_p) and the difference between line-of-sight velocities (Δv) (Ellison et al. 2008; Patton et al. 2013; Zuo et al. 2018), the current definition of the merger stage for galaxy pairs has several shortcomings. The projected separation (d_p) may not reveal the physical separation of member galaxies (Soares 2007) due to the projection effect. Furthermore, galaxy pairs with the same separation but at different merging stages could experience different interacting strengths (Torrey et al. 2012).

Recent integral field unit (IFU) surveys of nearby galaxies have revealed a possible connection between the asymmetry of gas kinematics with galaxy interactions (Barrera-Ballesteros et al. 2015; Bloom et al. 2018). Using the IFU data from Mapping Nearby Galaxies at APO (MaNGA) survey, Feng et al. (2020) investigated the kinematic asymmetry (\bar{v}_{asym}) of the ionized gas in a large sample of paired galaxies. Derived from H α velocity maps of galaxies (see details in Feng et al. 2020), the value of \bar{v}_{asym} describes the asymmetry of the velocity field contributed by the interaction-induced nonrotating motion. They find the star formation of paired galaxies with high kinematic asymmetries is significantly enhanced, while paired galaxies with low kinematic asymmetries show no significant enhancement of star formation rate (SFR) even at small projected separation. For pairs with high \bar{v}_{asym} , the enhancement of SFR shows a tight anti-correlation with projected separation. These findings suggest that the kinematic asymmetry is an effective indicator of galaxy mergers.

The enhancement of star formation during galaxy-galaxy interactions requires sustaining gas supply, which can be further investigated by observations of cold gas (e.g., HI gas) in galaxy pairs. In this work, we compile a major-merger galaxy pairs sample selected from the MaNGA survey to study the HI content of merging galaxies, adopting the kinematic asymmetry and projected separation as indicators of the merging stage. We compare the HI gas properties and star formation of the galaxy pair sample with a robustly matched control sample. Our study can provide better constraints on the HI gas fraction in merging galaxies and study the HI gas depletion/replenishment in clearly defined interacting stages.

2. Samples

The parent sample (Feng et al. 2020) consists of 578 isolated galaxy pairs, which are selected following these criteria: (1) the projected separation for member galaxies: $5 h^{-1} \text{ kpc} \leq d_p \leq 200 h^{-1} \text{ kpc}$, (2) the line-of-sight velocity difference: $|\Delta v| \leq 500 \text{ km s}^{-1}$, (3) each pair member only has one neighbor satisfying the above criteria, (4) at least one member galaxy of each pair has been observed in the MaNGA survey, and the member galaxy has more than 70% spaxels with H α emission at $S/N > 5$ within 1.5 effective radius (R_e), and (5) we only study star-forming galaxies ($\log(\text{sSFR}/\text{yr}^{-1}) > -11$) in this work. To study major-merger pairs, we require the mass ratio $M_1/M_2 < 3$, where M_1 and M_2 represent the stellar masses of primary galaxies and companions, respectively. The HI data used in this work are either obtained by our PI programs with FAST or extracted from the HI-MaNGA survey (Stark et al. 2021). Constrained with the above requirements, the final pair sample consists of 66 galaxy pairs with HI detections at $S/N > 5$.

Following Feng et al. (2020), we extract two subsamples from the pair sample based on their \bar{v}_{asym} values: low asymmetry ($0.007 < \bar{v}_{\text{asym}} < 0.029$), and high asymmetry ($0.029 < \bar{v}_{\text{asym}} < 0.316$). As revealed by recent simulations, paired galaxy after the

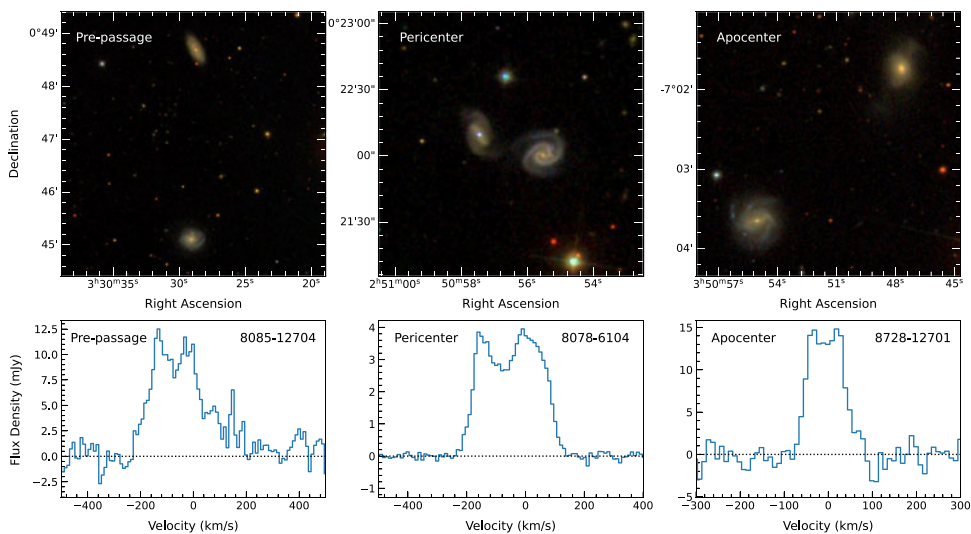


Figure 1. Examples of SDSS optical images and the corresponding H I line profiles of galaxy pairs at pre-passage, pericenter, and apocenter stages, respectively.

pericentric passage shows a more disturbed velocity field than that before the passage (Hung *et al.* 2016). Therefore, galaxy pairs with low \bar{v}_{asym} values are defined as pre-passage pairs, which indicates there are no significant interactions between member galaxies. Simulations suggest the physical separation constantly decreases before pericentric passage and increases when the paired galaxies are approaching apocenter (Torrey *et al.* 2012; Moreno *et al.* 2019). Hence, we use the projected separation (d_p) as a reference to distinguish the pericenter and apocenter stages of merging galaxy pairs. We define the high \bar{v}_{asym} -valued pairs with $d_p < 50 h^{-1}$ kpc to be at the stage of pericenter passage, and the high \bar{v}_{asym} -valued pairs with $d_p > 50 h^{-1}$ kpc are approaching the apocenter passage. In Figure 1, we present examples of the SDSS optical images and corresponding H I line profiles of galaxy pairs at pre-passage, pericenter, and apocenter stages, respectively. We have compiled a control sample of isolated star-forming galaxies from MaNGA to compare the effect of galaxy interactions on star formation and H I gas properties.

3. Results

3.1. H I Gas Properties

We detect 6 H I emission lines and 1 absorption line in FAST observations of 8 galaxy pairs. For each detected source, we estimate the H I mass. For galaxy pairs in the HI-MaNGA survey, we adopt the H I mass from the HI-MaNGA DR2 catalog (Stark *et al.* 2021). Adopting the derived H I mass ($M_{\text{H I}}$), we calculated the H I gas fraction ($f_{\text{H I}}$) and the star formation efficiency of H I gas ($\text{SFE}_{\text{H I}}$). The H I gas fraction $f_{\text{H I}}$ is defined as $f_{\text{H I}} = M_{\text{H I}}/M_{\star}$. The mean H I gas fraction of the pair sample in logarithm is $\log f_{\text{H I}} = -0.12 \pm 0.06$. In contrast, the mean H I gas fraction of the control sample ($\log f_{\text{H I}} = -0.03 \pm 0.02$) is higher than that of the pair sample, which indicates the control galaxies are more gas-rich. However, the $f_{\text{H I}}$ is tightly correlated to the global stellar mass (M_{\star}) for star-forming galaxies (Catinella *et al.* 2010), so we perform a galaxy-by-galaxy match between the pair sample and control sample in Section 3.2.

We use $\text{SFE}_{\text{HI}} = \text{SFR}/M_{\text{HI}}$ to describe the star formation efficiency of HI gas for galaxies in pairs and controls. The mean $\log(\text{SFE}_{\text{HI}}/\text{yr}^{-1})$ values are -9.80 ± 0.06 and -9.96 ± 0.02 for galaxies in pairs and controls, respectively.

3.2. HI Depletion and SFR Enhancement at Different Merger Stages

To compare the HI gas fraction and other properties of galaxies in the pair sample and control sample along the merger sequence, we calculate the “offset” quantities following the method of Ellison et al. (2015, 2018). We match each paired galaxy in stellar mass and redshift with at least five isolated galaxies in the control pool. The matched galaxies are required to satisfy the tolerance of $|\Delta \log(M_{\star}/M_{\odot})| < 0.2$ and $|\Delta z| < 0.01$ (Feng et al. 2020).

After matching the stellar mass and redshift, the offset of HI gas fraction, is calculated as

$$\Delta f_{\text{HI}} = \log f_{\text{HI, pair}} - \log \text{median}(f_{\text{HI, control}}), \quad (1)$$

where the $\log f_{\text{HI, pair}}$ is the HI gas fraction of paired galaxy, and the $\log \text{median}(f_{\text{HI, control}})$ represents the median HI gas fraction of its matched control galaxies in the logarithm scale. We apply the same method to compute the offsets of SFR (ΔSFR) and SFE_{HI} ($\Delta \text{SFE}_{\text{HI}}$). The mean HI gas fraction offset of the galaxy pair sample is $\Delta f_{\text{HI}} = -0.06 \pm 0.03$ dex, which indicates the average f_{HI} of paired galaxies is $\sim 15\%$ deficient compared to isolated galaxies. The SFR offset of the pair sample is $\Delta \text{SFR} = 0.09 \pm 0.05$ dex, suggesting the SFR of paired galaxies and isolated galaxies on average have no significant difference. The enhanced SFR ($\sim 23\%$) is only marginally detected with large uncertainty. The SFE_{HI} offset of the pair sample is 0.12 ± 0.06 dex, which indicates the average SFE_{HI} in galaxy pairs is marginally enhanced by $\sim 32\%$ compared with control galaxies.

We present our main results in Figure 2. The histograms of the offsets of different galaxy properties are shown in top panels of Figure 2, and lower panels show the mean values of each distribution. Our results suggest mild HI depletion occurs during the merging process, especially when pairs are at the pericenter stage. In Figure 2(a) and Figure 2(d), we plot the distributions of HI gas fraction offsets for each subsample. Compared to the controls, the mean values of each distribution indicate that on average the HI gas fraction of pairs is marginally decreased at pericenter and apocenter stages for 0.10 ± 0.05 dex and 0.05 ± 0.04 dex ($\sim 26\%$ and $\sim 12\%$, respectively). At the pre-passage stage, the HI gas fraction offset of galaxy pairs is $\Delta f_{\text{HI}} = -0.04 \pm 0.05$ dex, which is comparable to that of isolated galaxies. The cyan data points show the results of FIRE-2 simulation (Moreno et al. 2019), which predicts a $\sim 4\%$ enhancement of the cool gas mass on average during the galaxy-pair period. Comparing with their simulation results, our data indicate weak decreases of f_{HI} for pairs at pericenter and apocenter stages, respectively.

The offset of SFR reveals that the star formation is enhanced when galaxy pairs are encountering close interactions. In Figure 2(b), the ΔSFR in pairs during pericentric passage tends to distribute at positive values, which indicates enhanced SFR. As shown in Figure 2(e), on average the paired galaxies during pericenter passage have strong SFR enhancement $\Delta \text{SFR} = 0.42 \pm 0.11$ dex, and the mean ΔSFR values of paired galaxies during pre-passage and apocenter passage are -0.01 ± 0.10 dex and 0.04 ± 0.06 dex, respectively.

Similar to SFR, our data suggest paired galaxies at the pericenter stage present significantly enhanced SFE_{HI} . As shown in Figure 2(c), the distributions of $\Delta \text{SFE}_{\text{HI}}$ for each subsample are similar to those of ΔSFR . Our results in Figure 2(f) indicate that the average SFE_{HI} of paired galaxies during pericenter passage is significantly enhanced by

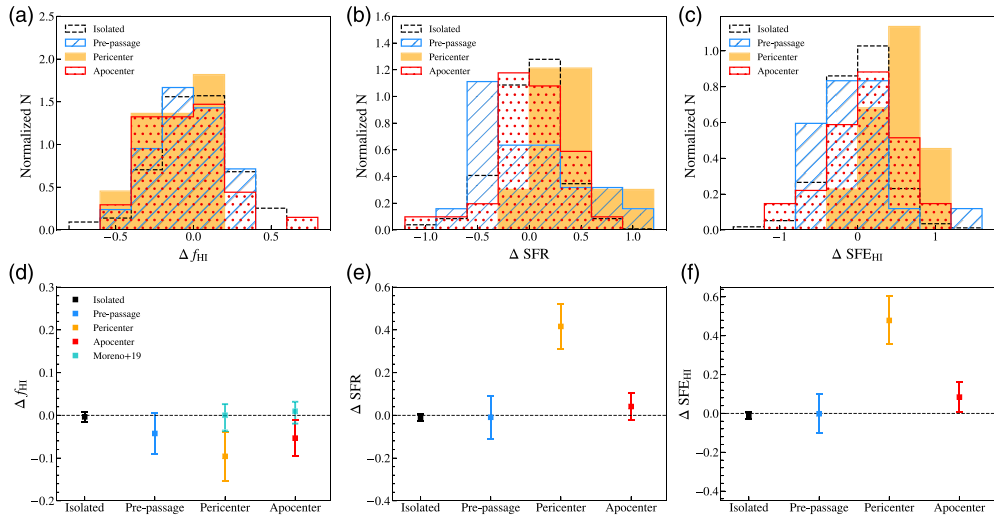


Figure 2. The top panels show histograms of different galaxy property offsets. Paired galaxies at different merger stages and the control sample are marked with blue, orange, red and black, respectively. (a) The distribution of Δf_{HI} . (b) The distribution of ΔSFR . (c) The distribution of $\Delta \text{SFE}_{\text{HI}}$. The middle panels show the mean value distributions for different galaxy property offsets. In each plot, the mean value is indicated by square point in the middle and the error of the mean as error bar for each distribution. (d) The mean value of Δf_{HI} of our results and the simulation results (cyan data points) from [Moreno et al. \(2019\)](#). (e) The mean value of ΔSFR . (f) The mean value of $\Delta \text{SFE}_{\text{HI}}$.

0.48 ± 0.12 dex. In contrast, the paired galaxies at the pre-passage stage shows no difference of the SFE_{HI} compared with the controls ($\Delta \text{SFE}_{\text{HI}} = 0.00 \pm 0.10$ dex). The mean SFE_{HI} offset of pairs at the apocenter stage is $\Delta \text{SFE}_{\text{HI}} = 0.08 \pm 0.08$ dex.

4. Discussions and Summary

For galaxy pairs at the pre-passage stage, there are no significant interactions between member galaxies. Therefore, the HI gas fraction, SFR, and SFE_{HI} of pairs are similar to that of isolated galaxies, which has been presented by our results (Figure 2).

During the pericentric passage, our analysis suggest that the member galaxies show significantly enhanced SFR (a factor of ~ 2.6), which is consistent with previous studies of close galaxy pairs ([Patton et al. 2013](#)). As revealed by previous CO observations of close pairs, the molecular gas fraction is also significantly enhanced and correlated to the enhancement of SFR ([Pan et al. 2018](#); [Violino et al. 2018](#); [Lisenfeld et al. 2019](#)). Due to external pressure, the enhancement of molecular gas fraction may originate from an accelerated transition from atomic to molecular gas, which can arise in the early stage of the merger ([Kaneko et al. 2017](#)). In this scenario, the moderate decrease of f_{HI} revealed by our work can be explained as HI gas depletion in fueling the H_2 reservoir. Furthermore, the enhanced molecular-to-atomic gas mass ratio in close interacting pairs ([Lisenfeld et al. 2019](#)) may lead to the significantly enhanced SFE_{HI} indicated by our data, considering the $\text{SFE}_{\text{HI}} = \text{SFE} \times (M_{\text{H}_2}/M_{\text{HI}})$, where the SFE is not enhanced compared with isolated galaxies ([Casasola et al. 2004](#); [Lisenfeld et al. 2019](#)). Alternatively, some recent observations of close pairs found small ($<$ a factor of 2) SFE enhancement ([Pan et al. 2018](#); [Violino et al. 2018](#)), which may also be able to drive the enhanced SFE_{HI} revealed by our data.

At the apocenter stage, our data suggest the HI gas fraction of pairs remains suppressed compared to isolated galaxies. Compared to pairs during the pericentric passage, the HI gas reservoir seems to be mildly replenished after strong interaction. This can be explained by the cooling of hot/warm gas from CGM (Moster et al. 2011; Tonnesen & Cen 2012), considering the interaction-induced shocks at the pericenter stage can be gradually alleviated when pairs are approaching the apocenter. As for SFR, the star formation of pairs at the apocenter stage is decreased relative to the previously enhanced SFR during pericentric passage. The decrease of SFR enhancement is in agreement with the previous result that galaxy pairs with large projected separations present weak SFR enhancement (Scudder et al. 2012; Patton et al. 2013). Simulations also suggest the merger-induced SFR enhancement is gradually decreased when the paired galaxies are approaching the apocenter (Moreno et al. 2019). As discussed above, the change of SFE_{HI} can be driven by SFE and M_{H_2}/M_{HI} . However, previous CO studies lack observations of pairs at the apocenter stage, which requires further CO observations of our pair sample to help determine the dominating factor for the observed suppression of SFE_{HI} enhancement.

We conclude that our study reveals marginal detection of the HI gas depletion during the galaxy-pair period of the merger. The suppressed HI gas fraction may originate from the gas consumption in fueling the enhanced H_2 reservoir of galaxy pairs. As a new method to use kinematic asymmetry as the indicator of galaxy interaction, we can further continue this study as more and more IFU data become available. Since our results are based on the global properties of galaxies in pairs, spatially resolved HI observations will help us further explore the interplay between galaxy interactions and the HI gas. Combining observations of the molecular gas for our sample, we will be able to build a complete picture of the cold gas evolution during mergers in the local universe.

References

- Barrera-Ballesteros J. K., et al., 2015, *A&A*, 582, A21
 Bloom J. V., et al., 2018, *MNRAS*, 476, 2339
 Casasola V., Bettoni D., Galletta G., 2004, *A&A*, 422, 941
 Catinella B., et al., 2010, *MNRAS*, 403, 683
 Cox T. J., Jonsson P., Somerville R. S., Primack J. R., Dekel A., 2008, *MNRAS*, 384, 386
 Di Matteo P., Combes F., Melchior A. L., Semelin B., 2007, *A&A*, 468, 61
 Ellison S. L., Patton D. R., Simard L., McConnachie A. W., 2008, *AJ*, 135, 1877
 Ellison S. L., Fertig D., Rosenberg J. L., Nair P., Simard L., Torrey P., Patton D. R., 2015, *MNRAS*, 448, 221
 Ellison S. L., Catinella B., Cortese L., 2018, *MNRAS*, 478, 3447
 Feng S., Shen S.-Y., Yuan F.-T., Riffel R. A., Pan K., 2020, *ApJL*, 892, L20
 Georgakakis A., Forbes D. A., Norris R. P., 2000, *MNRAS*, 318, 124
 Hani M. H., Sparre M., Ellison S. L., Torrey P., Vogelsberger M., 2018, *MNRAS*, 475, 1160
 Hibbard J. E., van Gorkom J. H., 1996, *AJ*, 111, 655
 Hung C.-L., Hayward C. C., Smith H. A., Ashby M. L. N., Lanz L., Martínez-Galarza J. R., Sanders D. B., Zezas A., 2016, *ApJ*, 816, 99
 Janowiecki S., Catinella B., Cortese L., Saintonge A., Brown T., Wang J., 2017, *MNRAS*, 466, 4795
 Kaneko H., Kuno N., Iono D., Tamura Y., Tosaki T., Nakanishi K., Sawada T., 2017, *PASJ*, 69, 66
 Lisenfeld U., Xu C. K., Gao Y., Domingue D. L., Cao C., Yun M. S., Zuo P., 2019, *A&A*, 627, A107
 Moreno J., et al., 2019, *MNRAS*, 485, 1320
 Moster B. P., Macciò A. V., Somerville R. S., Naab T., Cox T. J., 2011, *MNRAS*, 415, 3750
 Pan H.-A., et al., 2018, *ApJ*, 868, 132
 Pan H.-A., et al., 2019, *ApJ*, 881, 119

- Patton D. R., Torrey P., Ellison S. L., Mendel J. T., Scudder J. M., 2013, *MNRAS*, **433**, L59
- Satyapal S., Ellison S. L., McAlpine W., Hickox R. C., Patton D. R., Mendel J. T., 2014, *MNRAS*, **441**, 1297
- Scudder J. M., Ellison S. L., Torrey P., Patton D. R., Mendel J. T., 2012, *MNRAS*, **426**, 549
- Smith B. J., Campbell K., Struck C., Soria R., Swartz D., Magno M., Dunn B., Giroux M. L., 2018, *AJ*, **155**, 81
- Soares D. S. L., 2007, *AJ*, **134**, 71
- Stark D. V., et al., 2021, *MNRAS*, **503**, 1345
- Tonnesen S., Cen R., 2012, *MNRAS*, **425**, 2313
- Torrey P., Cox T. J., Kewley L., Hernquist L., 2012, *ApJ*, **746**, 108
- Violino G., Ellison S. L., Sargent M., Coppin K. E. K., Scudder J. M., Mendel T. J., Saintonge A., 2018, *MNRAS*, **476**, 2591
- Zuo P., Xu C. K., Yun M. S., Lisenfeld U., Li D., Cao C., 2018, *ApJS*, **237**, 2